Jan Perdulak – Dobroslav Kovac – Irena Kovacova – Matus Ocilka
– Andrii Gladyr – Dmytro Mamchur – Iurii Zachepa – Tibor Vince – Jan Molnar *

EFFECTIVE UTILIZATION OF PHOTOVOLTAIC ENERGY USING MULTIPHASE BOOST CONVERTER IN COMPARISON WITH SINGLE PHASE BOOST CONVERTER

The paper presents a novel concept of multiphase boost converter (MPBC) with high efficiency of energy conversion. The new topology of MPBC is compared with conventional single-phase boost converter (SPBC). It is shown that almost whole input energy from photovoltaic module entering to the proposed MPBC is utilized more effectively in comparison with conventional SPBC. This effective energy utilization is ensured by suitable algorithm of switches control. Modeling, simulation and experimental results are given. Subsequently the laboratory models of SPBC and MPBC were built and experimental results were obtained to confirm the simulation results. Also the control module of MPBC was designed, simulated and built to ensure the correct operation of proposed converter.

Keywords: *Multiphase boost converter, single phase boost converter, efficiency of energy conversion, photovoltaic.*

1. Introduction

Photovoltaic is the direct conversion of light into electricity in form of direct current electricity. Usually the *DC/DC* converters are used to convert this direct electrical power from one level to another.

There are many types of materials which are used to make of the PV modules. The main problem of these materials is low conversion efficiency which is usually moving from 5% (*a-Si*) to 25% – 30% (*GaAs*) [1]. Nowadays, the efficiency of the soft switching *DC/DC* converters is very high and it is moving around the 97%. But, on the other hand, the efficiency of energy conversion is not good in comparison with abovementioned converter efficiency.

This paper presents the novel concept of *MPBC* with high efficiency of energy conversion. The high efficiency of energy conversion is ensured by adding five more parallel legs to the conventional *SPBC*. The suitable algorithm of switches control in particular legs ensures that the almost whole *PV* output energy from the *PV* module is effective utilized.

2. Efficiency of energy conversion

Figure 1 explains the problem of efficiency of energy conversion. The impinging sun energy P_{IN_sun} is converted by *PV* module direct to the electric energy. According to the material from which *PV* module is built this conversion efficiency is moving from 5% (*a-Si*) to 30% (*GaAs*) [1] and [2]. The output *PV* energy P_{OUT_PV} is equal to the input energy to the converter P_{IN_con}.

Let us assume that *SPBC* is used to adjustment of input energy P_{IN_con} from one level to another.

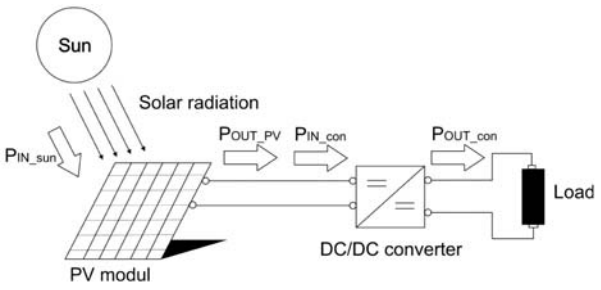

Fig. 1 Overview at efficiency of energy conversion

The function principle of conventional *SPBC* is well known. When the switch *S* is turned on the input energy starts to accumulate in form of magnetic field in the inductor *L*. This accumulated inductor energy with input energy (source energy) are delivered to the output *Z* after switch *S* is turned off. The average value of the output voltage $U_{Z(AV)}$ in continuous conduction mode (*CCM*) is:

* **Jan Perdulak[1], Dobroslav Kovac[1], Irena Kovacova[1], Matus Ocilka[1], Andrii Gladyr[2], Dmytro Mamchur[2], Iurii Zachepa[2], Tibor Vince[1], Jan Molnar[1]**
[1] Department of Theoretical Electrical Engineering and Electrical Measurement, Technical University of Kosice, Slovakia
[2] Department of Automatic Management and Electrical Drive, Kremenchuk Mykhailo Ostrohradskyi National University, Ukraine
E-mail: jan.perdulak@tuke.sk

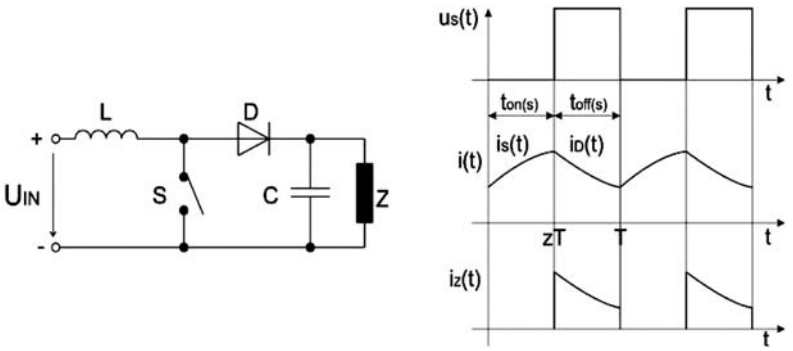

Fig. 2 Topology and theoretical waveforms of SPBC

$$U_{Z(AV)} = \frac{1}{1-z} U_{IN} \tag{1}$$

where duty cycle "z" is ratio between time when the switch S is turned on and the period T, $z = t_{on(s)}/T$. The theoretical waveforms and topology of conventional *SPBC* are shown in Fig. 2.

It can be seen that there exists a time interval within the period T when the energy delivered to the load Z is equal to zero. This is the main problem of conventional *SPBC* – effective utilization of input energy. We have to ensure that the input energy will be delivered to the load Z over the whole period T. We have to remove the time interval within the period T where the energy delivered to the load Z is zero. The another important fact is, that in case of unfavorable operating conditions of *PV* module, the *SPBC* is unable to obtain ist maximum power point (*MPP*)

It stands to reason that the efficiency of energy conversion is very low because we are unable to utilize the whole potential of input energy.

This is done by using the proposed *MPBC*, [3] and [4].

The three different efficiencies can be defined as:

The conversion efficiency of *PV* module η_{PV}:

$$\eta_{PV} = \frac{P_{OUT\_PV}}{P_{INsun}} \tag{2}$$

The converter efficiency η_{con}:

$$\eta_{con} = \frac{P_{OUTcon}}{P_{INcon}} \tag{3}$$

The efficiency of energy conversion η_E:

$$\eta_E = \frac{P_{OUTcon}}{P_{OUT\_PV(MPP)}} \tag{4}$$

where $P_{OUT\_PV(MPP)}$ is the instantaneous maximal output power of *PV* module for its certain operating conditions.

3. The proposed concept of MPBC

The proposed topology of *MPBC* is in Fig. 3a. The *MPBC* has, in comparison with the conventional *SPBC*, five more parallel legs with five inductors (L_2 – L_6), five rectifier diodes (D_2 – D_6) and five switches (S_2 – S_6).

This *MPBC* allows the effective utilization of energy delivered form the *PV* module. Appropriate control algorithm of switches allows converter to take the *PV* output energy by cooperation of all six parallel legs in every moment.

4. Principle of operation

The principle of operation of *SPBC* was mentioned above. This described process can be repeated six times because six parallel legs are presented in proposed *MPBC* which allows effective utilization of delivered energy from *PV* module.

The proposed *MPBC* has 6 operating cycles within each period. The corresponding operation waveforms are shown in Fig. 3b.

***Mode 1* (t_0 – t_1):** The switch S_1 (*leg A*) is turned on at the time t_0. The energy in form of magnetic field begins to accumulate in inductor L_1. The input current is closed in loop $+U_{IN} - L_1 - S_1 - -U_{IN}$. In this mode the switches S_5 (*leg E*) and S_6 (*leg F*) are in on-state. The input energy is delivered to the inductor L_5 and L_6 in particular legs, too. The switches S_2 and S_3 (leg C) are in off-state. The inductor energy W_{L2} and W_{L3} is delivered through diodes D_2 and D_3 to the load Z. The equivalent equations are:

The inductor voltages $u_{L1}(t)$, $u_{L5}(t)$ and $u_{L6}(t)$ are:

$$u_{L1}(t) = u_{L5}(t) = u_{L6}(t) = U_{IN} = L_{1(5,6)} \frac{di_{L1(5,6)}(t)}{dt} \tag{5}$$

The inductor voltage $u_{L2}(t)$, $u_{L3}(t)$ and $u_{L4}(t)$ are:

$$u_{L2}(t) = u_{L3}(t) = u_{L4}(t) = U_{IN} - U_{out} = \\ = L_{2(3,4)} \frac{di_{L2(3,4)}(t)}{dt} \tag{6}$$

The currents flow through inductors L_1, L_5, L_6 and switches S_1, S_5, S_6 are

$$i_{L1}(t) = i_{L5}(t) = i_{L6}(t) = i_{S1}(t) = i_{S5}(t) = \\ = i_{S6}(t) = \frac{1}{L_{1(5,6)}}\int_{t0}^{t1} u_{L1(5,6)}(t)dt + I_{L1(5,6)}(t_0) = \\ = \frac{U_{IN}}{L_{1(5,6)}}(t_1 - t_0) + I_{L1(5,6)}(t_0) \quad (7)$$

The currents flow through inductors L_2, L_3, L_4 and diodes D_2, D_3, D_4 are:

$$i_{L2}(t) = i_{L3}(t) = i_{L4}(t) = i_{D2}(t) = i_{D3}(t) = \\ = i_{D4}(t) = \frac{1}{L_{2(3,4)}}\int_{t0}^{t1} u_{L2(3,4)}(t)dt + I_{L2(3,4)}(t_0) = \\ = \frac{U_{IN} - U_{OUT}}{L_{2(3,4)}}(t_1 - t_0) + I_{L2(3,4)}(t_0) \quad (8)$$

The inductor current $i_{L1}(t)$ exponentially increases from the initial value I_{L1} to the maximum value I_{L1max} (reached at the time t_3) with time constant $\tau_1 = L_1/R$.

Mode 2* (t_1 - t_2)** and ***mode 3* (t_2 - t_3)** are the same as ***mode 1. Only other switches S_2 (*leg B*, *mode 2*) and S_3 (*leg C*, *mode 3*) are turned on, on-state S_1, S_6 (*leg A* and *leg F*, *mode 2*) and S_1, S_2 (*legs A* and *B*, *mode 3*) and off-state S_3, S_4 (*leg D* and *leg C*, *mode 2*) and S_4, S_5 (*legs D* and *E*, *mode 3*). The corresponding equations are the same. Only subscripts are changed.

***Mode 4* (t_3 - t_4):** The switch S_1 is turned off and S_4 is turned in the beginning of this mode at the time t_3. The inductor energy W_{L1} begins to deliver through diode D_1 to the load Z. The output current $i_Z(t)$ is enclosed in the loop L_1 - D_1 - Z - $-U_{IN}$ - $+U_{IN}$. The switches S_2 (leg B) and S_3 (leg C) are on-state and the input energy is delivered to the inductor L_2 and L_3. The switches S_5 (leg E) and S_6 (leg F) are in off-state. The inductor energy W_{L5} and W_{L6} is delivered through diodes D_5 and D_6 to the load Z. The equivalent equations are:

The inductor voltages $u_{L4}(t)$, $u_{L2}(t)$ and $u_{L3}(t)$ are

$$u_{L4}(t) = u_{L2}(t) = u_{L3}(t) = U_{IN} = L_{4(2,3)}\frac{di_{L4(2,3)}(t)}{dt} \quad (9)$$

The inductor voltages $u_{L1}(t)$, $u_{L5}(t)$ and $u_{L6}(t)$ are

$$u_{L1}(t) = u_{L5}(t) = u_{L6}(t) = U_{IN} - U_{out} = \\ = L_{1(5,6)}\frac{di_{L1(5,6)}(t)}{dt} \quad (10)$$

The currents flow through inductors L_4, L_2, L_3 and switches S_4, S_2, S_3 are

$$i_{L4}(t) = i_{L2}(t) = i_{L3}(t) = i_{S4}(t) = i_{S2}(t) = \\ = i_{S3}(t) = \frac{1}{L_{4(2,3)}}\int_{t3}^{t4} u_{L4(2,3)}(t)dt + I_{L4(2,3)}(t_0) = \\ = \frac{U_{IN}}{L_{4(2,3)}}(t_3 - t_4) + I_{L4(2,3)}(t_3) \quad (11)$$

The currents flow through inductors L1, L5, L6 and couple of diodes D1, D5, D6 are

$$i_{L1}(t) = i_{L5}(t) = i_{L6}(t) = i_{D1}(t) = i_{D5}(t) = \\ = i_{D6}(t) = \frac{1}{L_{1(5,6)}}\int_{t3}^{t4} u_{L1(5,6)}(t)dt + I_{L1(5,6)}(t_3) = \\ = \frac{U_{IN} - U_{OUT}}{L_{1(5,6)}}(t_4 - t_3) + I_{L1(5,6)}(t_3) \quad (12)$$

The inductor current $i_{L4}(t)$ exponentially increases with time constant $\tau_4 = L_4/R$.

Mode 5* (t_4 - t_5)** and ***mode 6* (t_5 - t_6)** are the same as ***mode 4. Only other switches S_5 (*leg E, mode 5*) and S_6 (*leg F, mode 6*) are turned on, on-state S_3, S_4 (*leg C* and *leg D, mode 5*) and S_4, S_5 (*legs D* and *E*, *mode 6*) and off-state S_1, S_2 (*legs A* and *B*, *mode 6*) and S_1, S_6 (*leg A* and *leg F, mode 5*). The corresponding equations are the same. Only subscripts are changed.

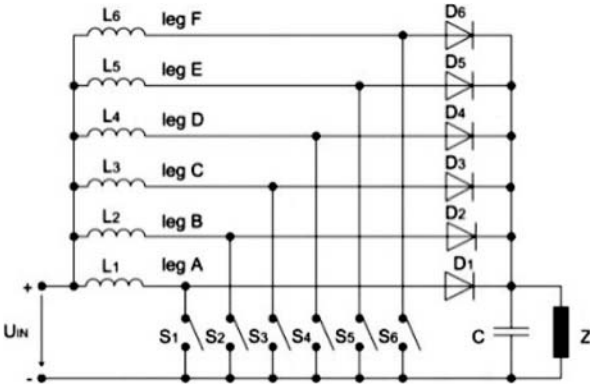

a)

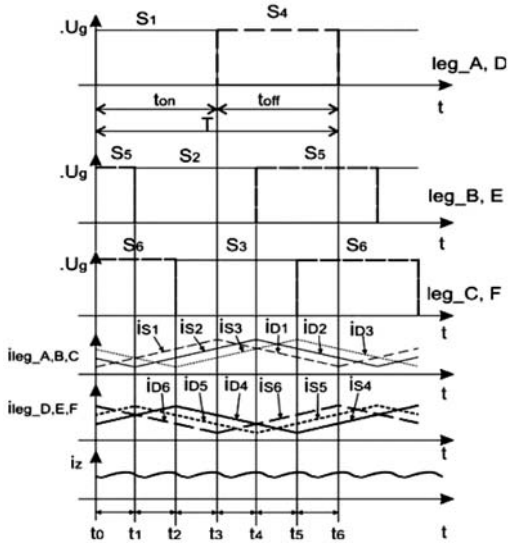

b)

Fig. 3 The proposed topology and theoretical waveforms of MPBC

5. Simulation Results

The simulation models of *MPBC* and *SPBC* shown in Fig. 4 were created in simulation environment OrCAD Capture CSI to verify its theoretical properties. The power MOSFET transistors were used as switches. The two *DC* voltage sources were used to simulate output photovoltaic voltage *UPV* and battery voltage U_{bat}. Parameters:

switching frequency $f_S = 50$ kHz,
output voltage $U_{bat} = 14$ V,
inductance $L = L_1 = L_2 = L_3 = L_4 = L_5 = L_6 = 100$uH

Three different levels of input voltage U_{PV} were set to compare the properties of simulation models of *MPBC* and *SPBC*. The tested values of input voltage were $U_{PV} = \{2\text{ V}, 6\text{ V}, 12\text{ V}\}$.

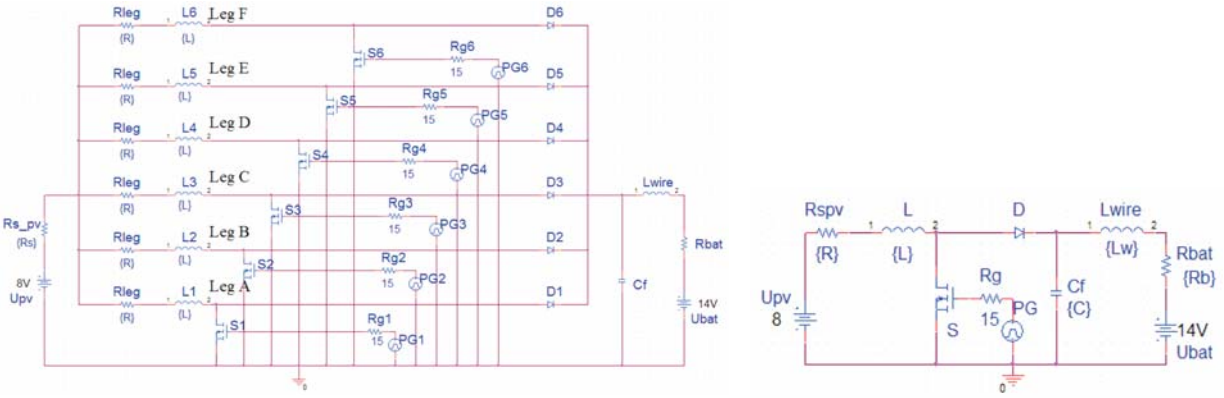

Fig. 4 Simulation models of proposed MPBC a) and conventional SPBC b)

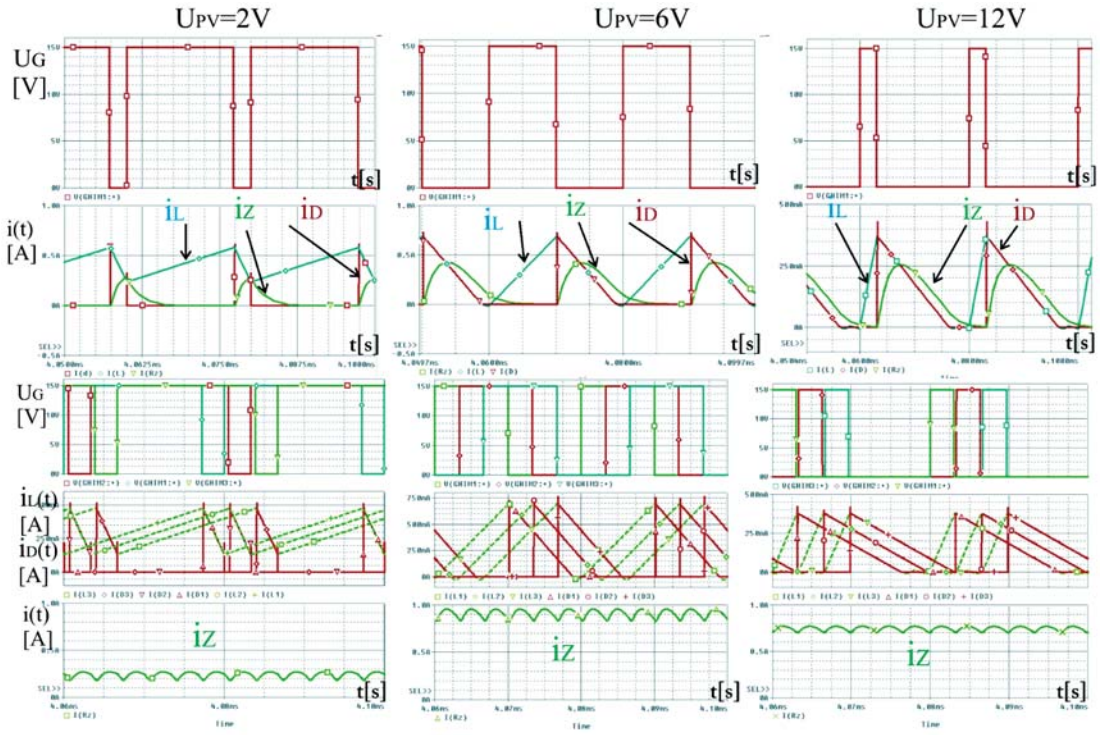

Fig. 5 Simulation comparison of basic properties of SPBC (upper part) and MPBC (lower part)

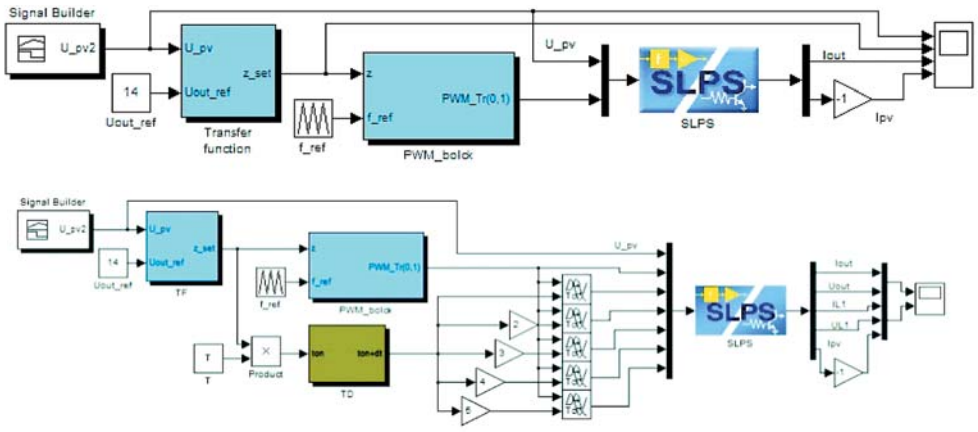

Fig. 6 Simulink models of control structure of SPBC (upper part) and conventional MPBC (lower part)

Figure 5 shows gate voltage U_G, inductor current $i_L(t)$, diode current $i_D(t)$, and load current $i_Z(t)$ at the different value of input voltage U_{PV}. In can be seen that the *MPBC* works in comparison with *SPBC* in *CCM* for whole range of input voltage U_{PV} except the minimum value $U_{PVmin} = 2$ V. The load current $i_Z(t)$ is sum of currents in particular legs which delivers its energy to the load *Z*. The waveforms of three legs of *MPBC* are displayed for lucidity.

Control structures created in Simulink environment are shown in Fig. 6, [5]–[7]. For this purpose the *PSpice SLPS* (SimuLink PSpice) simulation environment was used. This environment supports the substitution of an actual Simulink block with an equivalent analog PSpice electrical circuit. The simulation models of *SPBC* and *MPBC* are completely included to the simulink model control design by means of *SLPS* block.

Figures 7a and 8a show overall view of load current $i_Z(t)$, inductor current $i_L(t)$, input voltage U_{PV} and duty cycle z of *SPBC* and *MPBC*. From the detailed analysis (Figs. 7b, 7c and 8b) it is clear that the *MPBC* works in comparison with SPBC in *CCM* for the whole range of input voltages U_{PV} except the minimum value $U_{PVmin} = 2$ V.

6. Experimental results

The laboratory models of *SPBC* and proposed *MPBC* were built and tested to verify the theoretical assumptions and simulation results. The laboratory model of control structure of *MPBC* was built and connected to the converter to generate corresponding gate signals for transistors in particular legs. Figure 9 shows the overall view connection of converter with designed control.

The *DC* regulated voltage source was used to simulate different operating conditions and thus different levels of output *PV* voltage U_{PV}. The battery was used as a load *Z*.

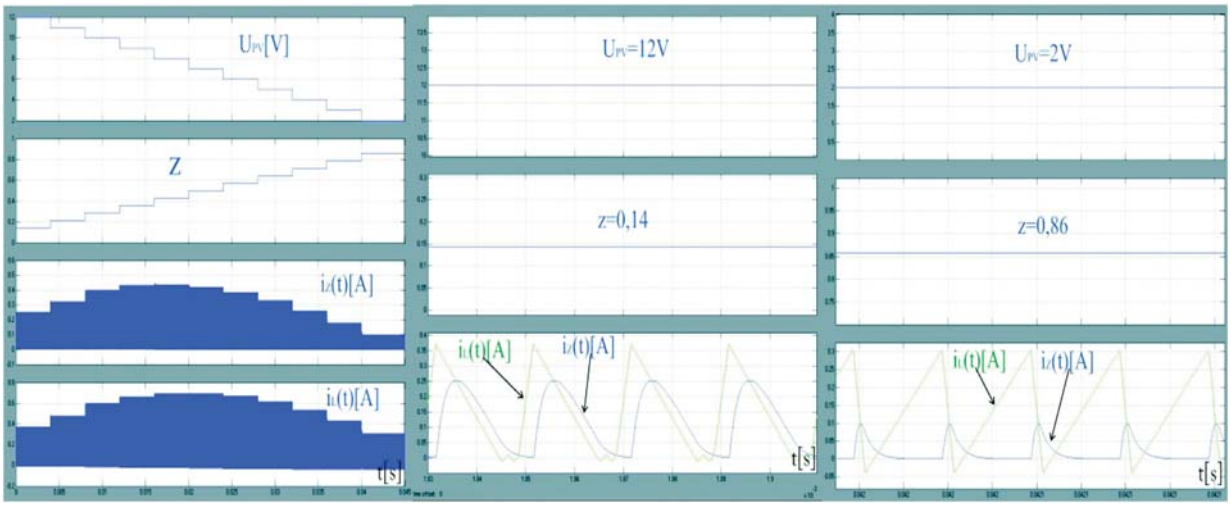

a) *b)* *c)*

Fig. 7 Waveforms of photovoltaic voltage UPV, duty cycle z, inductor current iL(t) and load current iZ(t) of SPBC

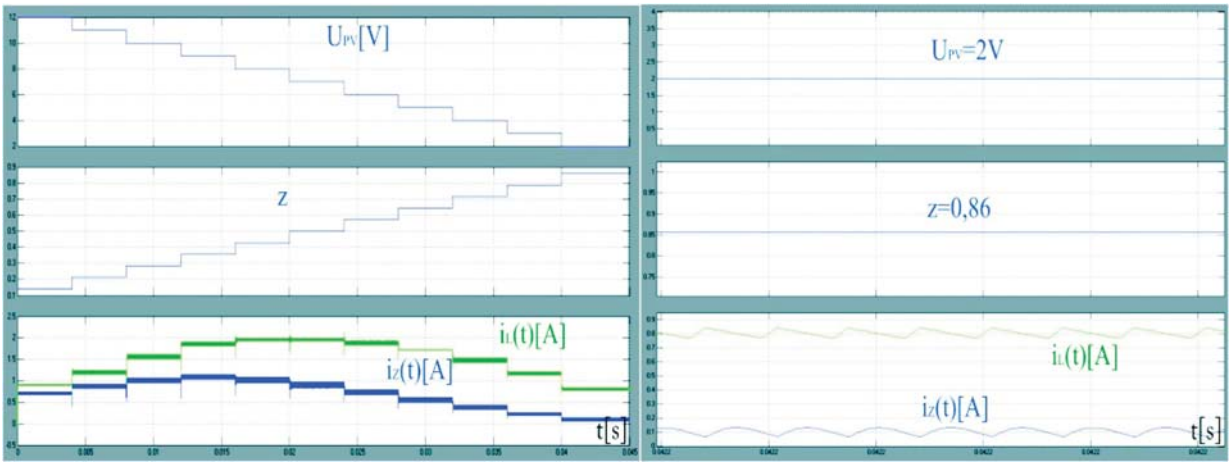

a) *b)*

Fig. 8 Waveforms of photovoltaic voltage U_{PV}, duty cycle z, inductor current $i_L(t)$ (leg A) and load current $i_Z(t)$ of MPBC

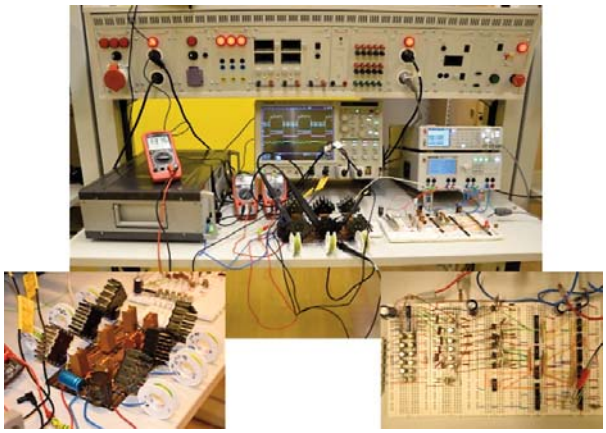

Fig. 9 Laboratory model of MPBC with control

Figures 10 and 11 show input voltage U_{PV}, gate voltage U_G, input current I_{PV} and load current $i_Z(t)$, of *SPBC* and *MPBC*. It is clear that the load current $i_Z(t)$ is continually delivered to the load *Z*. Even if input voltage U_{PV} is set to the minimum value 4 V the maximum input current I_{PV_max} is taken from the input voltage source. This is another important fact in comparison with *SPBC*. The laboratory model of proposed *MPBC* works in discontinuous conduction mode at the U_{PV} = 4V in comparison with simulation model. This is because the real components were used in comparison with the simulation model where many of parasitic and physical properties cannot be taken into account.

7. Comparison of efficiency of energy conversion

Efficiency of energy conversion η_E can be defined as a ratio of output converter energy P_{OUTcon} to the maximum output energy $P_{OUT\_PV(MPP)}$, of *PV* module which it is able to deliver under the given operating conditions. It is evident, that the efficiency of energy conversion η_E of *MPBC* is several times higher in comparison with *SPBC*, Fig. 12, for the whole range of operating conditions. The low efficiency of energy conversion η_E of *SPBC* results from its principle of operation. The *SPBC* operates in pulse mode so only a portion of its input energy is delivered to output. The *PV* module operates

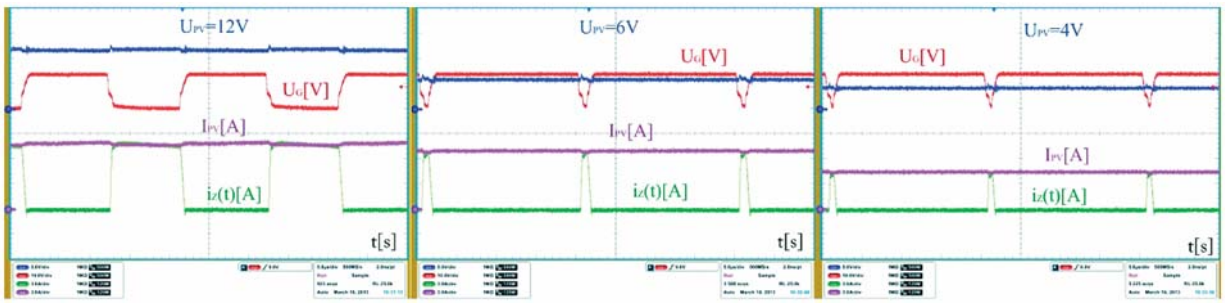

Fig. 10 Waveforms of photovoltaic voltage U_{PV}, duty cycle z, photovoltaic current $i_Z(t)$ and load current $i_Z(t)$ of SPBC

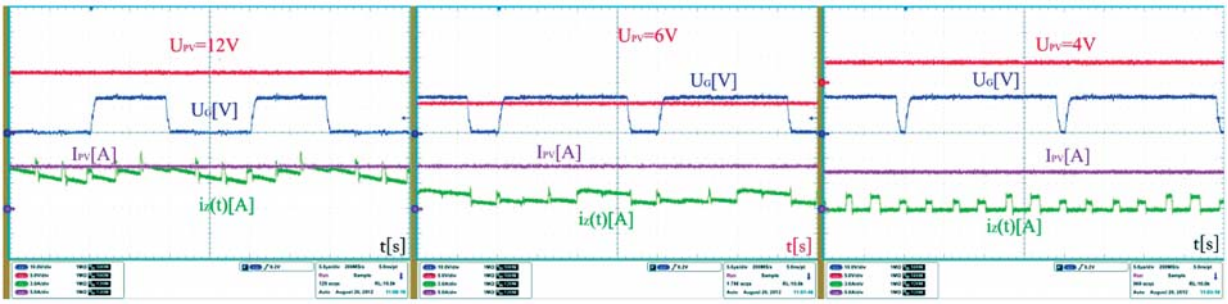

Fig. 11 Waveforms of photovoltaic voltage U_{PV}, duty cycle z, photovoltaic current $i_Z(t)$ and load current $i_Z(t)$ of MPBC

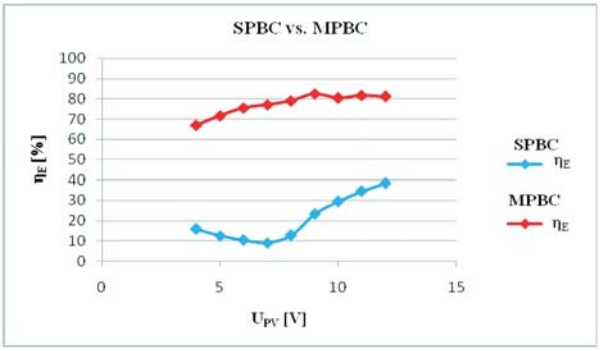

Fig. 12 Comparison of efficiency of energy conversion

in *MPP* point for whole range of operating conditions, or more precisely, for the whole range of input photovoltaic voltage U_{PV} when the *MPBC* is used.

8. Conclusion

The most popular material used to make the solar cell is silicium (*Si*). The *Si* is also one of major factors in long-term energy recovery and high cost of *PV* modules. One way to reduce the long –term energy and financial recovery is to use the proposed *MPBC*. The *MPBC* works with high efficiency of energy conversion in comparison with *SPBC*. The *MPBC* continually delivers the input source energy to the load Z using six parallel phases. In this case, the time interval when the output energy is equal to zero is removed. The *MPBC* ensures that the PV module is operating in the maximum power point for whole range of its operating conditions, so we can effectively utilize the output *PV* energy.

Acknowledgement

The paper has been prepared under the support of the Slovak grant project KEGA No. 005TUKE-4/2012.

References

[1] MAH, O.: *Fundamentals of Photovoltaic Materials.* National Solar Power Research Institute, Inc., 1998, pp.10.
[2] TURCEK, J., HRASKO, M., ALTUS, J.: Photovoltaics in Present Days and their Coexistence with Power System. *Communications - Scientific Letters of the University of Zilina*, No. 2A, pp.109–113, 2011.
[3] KOVAC, D., KOVACOVA, I.: Patent application No. 00150-2010.
[4] KOVAC, D., KOVACOVA, I.: Patent application No. 00001-2011.
[5] DOBRUCKY B., BENOVA, M., FRIVALDSKY, M., PRAZENICA, M.: Choosing Modulation Strategies for 2-Stage Combine LLC - and Direct Converter - Modelling, Simulation, Application. *Communications - Scientific Letters of the University of Zilina,* No. 2A, pp. 25–31, 2011.
[6] KOVAC, D., KOVACOVA, I., PERDULAK, J., VINCE, T., MOLNAR, J.: Patent app. No. 00097-2011.
[7] KOVAC, D., KOVACOVA, I., PERDULAK, J., VINCE, T., MOLNAR, J.: Patent app. No. 00008-2012.